

## Four-body model of the four-nucleon system

A. C. Fonseca

*Department of Physics and Astronomy, University of Maryland, College Park, Maryland 20742*

(Received 16 June 1978)

Using a nonrelativistic field theoretic formalism a soluble model of the four-nucleon system is developed and solved numerically. Two- and three-body scattering proceeds through intermediate quasiparticles and the resulting  $T$  matrices are separable in momentum space and satisfy two- and three-body unitarity. The  $2+2$  subamplitudes are treated exactly by the convolution method. The resulting four-body equations reduce to single variable integral equations following partial wave decomposition and can be solved numerically by rotation of contour together with matrix inversion. A complete phase shift calculation is performed for the isospin triplet interaction. The differential cross sections for all two-to-two processes initiated by  $p+{}^3\text{He}$ ,  $n+{}^3\text{H}$  and  $d+d$  are compared with experiment for energies up to 25 MeV in the center of mass. Total elastic and reaction cross sections for the processes initiated by  $n+{}^3\text{H}$  are also calculated and compared with experimental data.

[NUCLEAR REACTIONS Four-body calculation of  ${}^3\text{H}(n, n){}^3\text{H}$ ,  ${}^3\text{He}(p, p){}^3\text{He}$ ,  ${}^2\text{H}(d, d){}^2\text{H}$ ,  ${}^2\text{H}(d, n){}^3\text{He}$ ]

### I. INTRODUCTION

After the work of Faddeev in the three-body problem<sup>1</sup> substantial progress was achieved in the formulation of connected kernel integral equations for the  $n$ -body problem.<sup>2</sup> Unlike the Lippmann-Schwinger equations, they have the advantage that after iteration their kernel becomes a compact operator. The method of integral equations has therefore been used almost exclusively to carry out quantitative four-body calculations for the four-nucleon problem. Although these equations are, at least in principle, solvable by standard methods, their complexity is so great that few scattering solutions<sup>3-5</sup> exist for realistic two-body potentials. The main difficulty involves the need to use the off-shell  $1+3$  and  $2+2$  subamplitudes as input to the four-body equations. Even if two-body separable potentials are used between pairs, the resulting subamplitudes are nonseparable in momentum space, and this leads to multi-variable integral equations that are extremely time consuming to solve numerically even in the fastest computers currently available.<sup>6</sup> If a separable approximation to the kernel of the four-body equations is introduced, it is possible to reduce them to one vector variable in intermediate states which after partial wave decomposition become single variable integral equations. This method has been used extensively in the four-nucleon problem to obtain bound states or threshold scattering results<sup>8-10</sup> because in that energy region a small number of terms is sufficient to obtain accurate solutions. On the contrary, in the scattering region, the number of separable terms per subamplitude that is required to in-

clude, grows fast as the energy increases beyond rearrangement and breakup thresholds.<sup>4</sup> In addition to the difficulties inherent to the singularity structure of the four-body kernel that are common to any calculation method, this leads to very large sets of coupled equations that are also hard and time consuming to solve.

In view of the present state of the art we find it convenient to formulate a four-body model of the four-nucleon system that exhibits as many features of the experimental problem as possible, and whose solution in the scattering region may be obtained with considerably less numerical effort than a more exact formalism would allow. In a previous work<sup>11</sup> we used the field theoretic method of Amado<sup>12</sup> to formulate a soluble model for four identical particles and studied a spinless version of the four-nucleon problem. Now the theory is generalized to include spin and isospin effects so that a more realistic approach to the four-nucleon system may be attempted. As before, the long range Coulomb force will be disregarded.

The elementary particle of the present model, the nucleon, is named  $N$  and has both spin and isospin  $\frac{1}{2}$ . We follow the nuclear physics convention and assign isospin projection  $+\frac{1}{2}$  to the neutron and  $-\frac{1}{2}$  to the proton. In the two-body sector of the model two quasiparticles  $d$  and  $\phi$  are introduced with  $s$ -wave coupling to two  $N$ 's. Two-body  $NN$  scattering proceeds through the  $d$  (deuteron) each time a spin triplet pair interacts and through the  $\phi$  whenever a spin singlet pair interacts. The  $d$  is, therefore, a physical particle with spin 1 and is isospin 0 and the  $\phi$  an unphysical particle with spin 0 and isospin 1. In the three-body sector, both the total spin and the to-

tal isospin have two possible values,  $\frac{1}{2}$  and  $\frac{3}{2}$ , and the dynamical equations that describe three-body bound states and scattering states are those of Aaron, Amado, and Yam<sup>13</sup> (AAY). Since no tensor or spin orbit force is included, both the total angular momentum and total spin are conserved and for the total three-body orbital angular momentum  $l=0$ , there are three independent amplitudes that can be characterized by their spin and isospin according to Table I. We have called them  $(D, D)$ ,  $(Q, D)$  and  $(D, Q)$  where  $D$  stands for doublet and  $Q$  for quartet. As in the spinless model<sup>11</sup> an approximation to the AAY exact three-body amplitudes is developed. It is assumed that the three-body problem of interest is dominated by the three  $l=0$  amplitudes  $(D, D)$ ,  $(Q, D)$ , and  $(D, Q)$  and three quasiparticles meant to approximate three-body scattering in each of these states are introduced. In the absence of a better designation they are called  $t$ ,  $t'$ , and  $t''$  with spin and isospin assigned according to Table I. Since the short range forces are charge independent and the long range Coulomb force has been disregarded, the  $t$  represents  ${}^3\text{H}$  or  ${}^3\text{He}$  depending on whether its isospin projection is  $\frac{1}{2}$  or  $-\frac{1}{2}$ . The  $t$  is coupled to both  $N+d$  and  $N+\phi$  and the renormalized parameters of the interactions are chosen such that equal mixtures of  $N+d$  and  $N+\phi$  are present in the wave function of the  $t$ . The  $t'$  and the  $t''$  are unphysical particles coupled exclusively to  $N+d$  and  $N+\phi$ , respectively. Proceeding to the four-body sector we obtain after partial wave decomposition, one-dimensional integral equations for the processes  $n^3\text{He} \rightarrow n^3\text{He}$ ,

TABLE I. The three independent three-body amplitudes with orbital angular momentum  $l=0$ .

Amplitudes	Spin	Isospin	Quasiparticle
$(D, D)$	$\frac{1}{2}$	$\frac{1}{2}$	$t$
$(Q, D)$	$\frac{3}{2}$	$\frac{1}{2}$	$t'$
$(D, Q)$	$\frac{1}{2}$	$\frac{3}{2}$	$t''$

$n^3\text{He} \rightarrow p^3\text{H}$ , and  $n^3\text{He} \rightarrow dd$ ,  $n^3\text{H} \rightarrow n^3\text{H}$ , as well as for  $dd \rightarrow n^3\text{He}$  and  $dd \rightarrow p^3\text{H}$ . Detailed numerical calculations indicate that the total cross sections obtained from unitarity for 2-3 processes in the three-body sector and for 2-3 and 2-4 processes in the four-body sector are non-negative and thus we find that our three-body approximation, which involves the neglect of certain classes of graphs, leads to no gross violation of unitarity.

In Sec. II we describe the two- and three-body amplitudes of the model. In Sec. III the four-body equations for all 2-2 processes are formulated, and in Sec. IV the results obtained from the solution of our equations are compared with experiment. Some conclusions are given in Sec. V.

## II. TWO- AND THREE-BODY AMPLITUDES

As in Aaron, Amado, and Yam three-nucleon model<sup>13</sup> we allow for an s-wave two-body  $N-N$  interaction that is described by the following spin and isospin dependent unrenormalized Hamiltonian ( $\hbar = 2m_n = 1$ ):

$$H = \sum_{s,i} \sum_{\vec{k}} (\vec{k}^2) N_{s,i}^\dagger(\vec{k}) N_{s,i}(\vec{k}) + \sum_{\substack{\Sigma, \Theta \\ \sigma, \theta}} \sum_{\vec{k}} (-\epsilon_\nu^{(0)} + \frac{1}{2}\vec{k}^2) [D_{\sigma, \theta}^{\Sigma, \Theta}(\vec{k})]^\dagger D_{\sigma, \theta}^{\Sigma, \Theta}(\vec{k}) \\ + \left[ \sum_{\text{all } \vec{q}, \vec{Q}} (1/\sqrt{2}) \gamma_\nu^{(u)} f_\nu(q) \langle \frac{1}{2} s_1 s_2 | \Sigma \sigma \rangle \langle \frac{1}{2} i_1 i_2 | \Theta \theta \rangle D_{\sigma, \theta}^{\Sigma, \Theta}(\vec{Q}) N_{s_1, i_1}^\dagger(\frac{1}{2}\vec{Q} - \vec{q}) N_{s_2, i_2}^\dagger(\frac{1}{2}\vec{Q} + \vec{q}) + \text{H.c.} \right] \quad (1)$$

where  $\vec{q}$  and  $\vec{Q}$  are the relative and total momenta of the two interacting particles. The first Clebsch-Gordon coefficient refers to spin and the second to isospin.  $\nu$  is either  $d$  or  $\phi$  depending on total spin and isospin of the pair interaction. Both  $D$  and  $N$  are field operators; the  $D$ 's obey the usual commutation relations suitable for bosons,

$$[D_{\sigma, \theta}^{\Sigma, \Theta}(\vec{k}), D_{\sigma', \theta'}^{\Sigma', \Theta'}(\vec{k}')] = \delta_{\vec{k}\vec{k}'} \delta_{\Sigma\Sigma'} \delta_{\Theta\Theta'} \delta_{\sigma\sigma'} \delta_{\theta\theta'}; \quad (2)$$

and the  $N$ 's obey the anticommutation relations appropriate to fermions,

$$\{N_{s,i}(\vec{k}), N_{s',i'}^\dagger(\vec{k}')\} = \delta_{\vec{k}\vec{k}'} \delta_{ss'} \delta_{ii'}. \quad (3)$$

All subscripts and superscripts referring to spin or isospin obey the following convention: Upper-

case letters are meant to designate the quantum numbers of spin and isospin, while lower case letters refer to projection quantum numbers; the greek alphabet is used for integer values, and the latin alphabet for half-integer values; the first symbol always refers to spin quantum numbers while the second to isospin quantum numbers.

The two-body scattering amplitudes resulting from (1) have been graphically represented in Fig. 1(a) and have a separable form in momentum space. Due to the Pauli exclusion principle two-body  $NN$  scattering is characterized by two independent s-wave amplitudes. They are

$$\langle \vec{k}' | T^{l,0}(E) | \vec{k} \rangle = \gamma_d^2 f_d(k) \tau_d(E + \epsilon_d) f_d(k'), \quad (4)$$

for a spin triplet pair and

$$\langle \vec{k}' | T^{0,1}(E) | \vec{k} \rangle = \gamma_{\phi}^2 f_{\phi}(k) \tau_{\phi}(E) f_{\phi}(k'), \quad (5)$$

for a spin singlet pair. Both the  $d$  particle and  $\phi$  particle propagators,  $\tau_d$  and  $\tau_{\phi}$ , are discussed in Appendix A and represent sums of self-energy bubbles. Each interaction is characterized by a coupling constant  $\gamma$  and a vertex function  $f(k)$ . The triplet interaction is also characterized by the wave function renormalization constant  $Z_d$  that takes on the range of values  $0 \leq Z_d \leq 1$ . The renormalized parameters of the interaction in each of these channels are chosen to fit the low energy triplet and singlet nucleon-nucleon data and their values are discussed in Appendix A.

If we move to the three-body sector we obtain a set of equations that describe particle quasi-particle scattering and that have already been studied by AAY.<sup>13</sup> The  $N\nu \rightarrow N\nu'$  ( $\nu, \nu' = d$  or  $\phi$ ) scattering amplitudes satisfy the integral equation depicted in Fig. 2. In each partial wave the equation reads

$$\begin{aligned} T_{\nu\nu'}^{UVI}(k', k; E) &= \Lambda_{\nu\nu'}^{UV} \mathfrak{B}_{\nu\nu'}^I(k', k; E) \\ &+ \sum_{\nu''=d, \phi} \int_0^{\infty} \frac{n^2 dn}{2\pi^2} \Lambda_{\nu\nu''}^{UV} \mathfrak{B}_{\nu''\nu'}^I(k', n; E) \\ &\times \tau_{\nu''}(E + \epsilon_{\nu''} - \frac{3}{2}n^2) T_{\nu''\nu'}^{UVI}(n, k; E), \quad (6) \end{aligned}$$

where  $\mathfrak{B}_{\nu\nu'}^I$  is the single  $N$ -exchange Born term and  $\Lambda_{\nu\nu'}^{UV}$  are the well-known three-body spin-isospin recoupling coefficients.<sup>13</sup> Since no tensor or spin-orbit force is included, for each value of  $l$  there are three independent amplitudes whose spin  $U$  and isospin  $V$  take on the values  $(\frac{1}{2}, \frac{1}{2})$ ,  $(\frac{3}{2}, \frac{1}{2})$ , and  $(\frac{1}{2}, \frac{3}{2})$ . The number of coupled equations

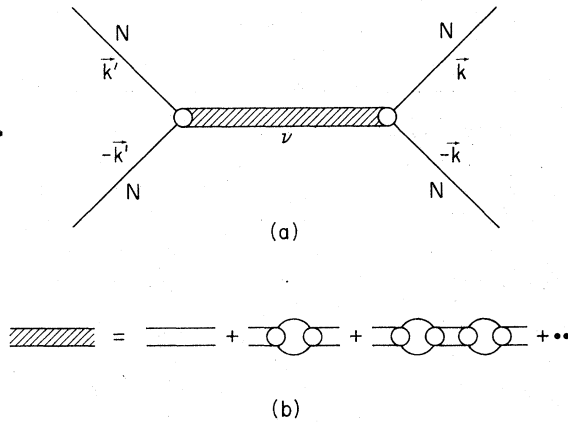


FIG. 1. (a) Graphical representation of the  $NN$  scattering amplitude.  $\nu$  is either  $d$  or  $\phi$  depending on the spin-isospin quantum numbers of the channel interaction. (b) First few terms in an expansion of the  $\nu$ -particle propagator.

depends on the values of  $U$  and  $V$ . For  $U = V = \frac{1}{2}$  both  $Nd$  and  $N\phi$  channels are included while for  $U = \frac{3}{2}, V = \frac{1}{2}$  only the  $Nd$  channel contributes. The  $N\phi$  channel is solely responsible for the  $U = \frac{1}{2}, V = \frac{3}{2}$  amplitude.

To proceed to the four-body problem with no further approximation would lead to the numerical difficulties inherent in multivariable integral equations, so that we insert our three-body approximation at this point. Unlike most of the previous work in the four-body problem<sup>3,4,8-10</sup> no attempt is made to expand the exact three-body amplitudes in a complete set of separable terms. Since the number of terms needed to obtain accurate results in the four-body sector grows fast<sup>4</sup> as the center-of-mass energy increases beyond rearrangement and breakup thresholds, such procedure would lead to a large number of coupled equations in the four-body problem and also to increasing difficulty in handling the singularities of the four-body kernel. Instead a model three-body amplitude is formulated that has the same analytical structure (poles and cuts) as the exact amplitude but contains some adjustable parameters that allow for some flexibility in fitting the on-shell three-body data. Our aim is to retain the simplicity that results whenever each independent three-body amplitude is described by a single separable term together with the ability to compensate for the suppression of higher order terms. For that purpose we proceed as in the spinless model<sup>11</sup> and introduce the following unrenormalized interaction Hamiltonian:

$$\begin{aligned} H_{N\nu}^I &= \sum_{\text{all}} \sum_{\vec{q}} \lambda_{\nu y} g_{\nu y}(\vec{q}) \langle \frac{1}{2} \Sigma s \sigma | U u \rangle \langle \frac{1}{2} \Theta i \theta | V v \rangle \\ &\times [T_{u\nu}^{UV}(\vec{q})]^t D_{\sigma\theta}^{2,0}(\frac{2}{3}\vec{Q} - \vec{q}) \\ &\times N_{s,t}(\frac{1}{3}\vec{Q} + \vec{q}) + \text{H.c.}, \quad (7) \end{aligned}$$

where  $\nu$  is either  $d$  or  $\phi$  and  $y$  is  $t, t'$ , or  $t''$  depending on the total spin and isospin of the channel interaction. The elementary particle in our model, the  $N$ , now couples in  $s$  wave to  $d$  or (and)  $\phi$  to generate  $t, t'$ , or  $t''$  with spin and isospin assigned according to Table I. It is therefore assumed that the three-body problem of interest can be characterized by the three  $l=0$  three-body amp-

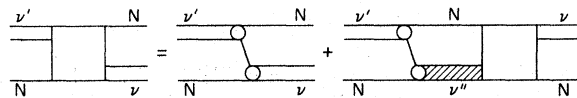


FIG. 2. Graphical representation of the integral equation for  $N\nu \rightarrow N\nu'$  amplitude (square) as described by Aaron, Amado, and Yam (Ref. 13).  $\nu$  and  $\nu'$  are either  $d$  or  $\phi$ .

litudes ( $D, D$ ), ( $Q, D$ ), and ( $D, Q$ ). The quasiparticles  $t$ ,  $t'$ , and  $t''$  are meant to approximate three-body scattering in each of these states. As in a previous work<sup>11</sup> the approximate three-body amplitudes do not include all possible diagrams that are consistent with both (1) and (7). We neglect all particle-exchange contributions and retain only the subclass of graphs that involve intermediate  $t$ 's as well as  $Nd$  or  $N\phi$  bubbles in intermediate states. According to our approximation,  $Nd$  scattering proceeds exclusively in  $s$  wave through the  $t$  for a state of total spin  $\frac{1}{2}$ , and through the  $t'$  for a state of total spin  $\frac{3}{2}$ . Since the  $\phi$  is an unphysical particle,  $N\phi$  scattering does not take place as an on-shell three-body process, but in the four-body sector of our model, virtual  $N\phi$  scattering will proceed exclusively in  $s$ -wave through  $t$  or  $t''$  depending on whether the total isospin of the three-body state is  $\frac{1}{2}$  or  $\frac{3}{2}$ . The three-body amplitudes of our model have been depicted in Fig. 3(a) and have a separable form in momentum space. In a representation in which the total spin and the total isospin of the channel is specified they may be written as

$$\langle \vec{k}' | T_{\nu\nu'}^{UV}(E) | \vec{k} \rangle = \lambda_{\nu y} g_{\nu y}(k') \tau_y(E + \epsilon_y) \times \lambda_{\nu y} g_{\nu y}(k), \quad (8)$$

where  $\tau_y$  is one of the three-particle propagators described in Appendix B. The spin  $U$  and isospin  $V$  of the intermediate quasiparticle plays the role of the total spin and total isospin of the channel since the interaction must proceed through this state. Since the  $t$  is coupled to both  $N+d$  and  $N+\phi$ , for  $U=V=\frac{1}{2}$  we have a two-channel process as in Eq. (6). Each interaction is characterized by a coupling constant  $\lambda$  and a vertex function  $g(k)$  which for simplicity is assumed to be energy independent. In addition to the wave function renormalization constant  $Z_t$  of the  $t$  that takes on the range of values  $0 \leq Z_t \leq 1$ , the ( $D, D$ ) interaction is also characterized by the percentage of  $N+d$  and  $N+\phi$  that is present in the wave function of the  $t$ . Due to the field theoretic nature of the

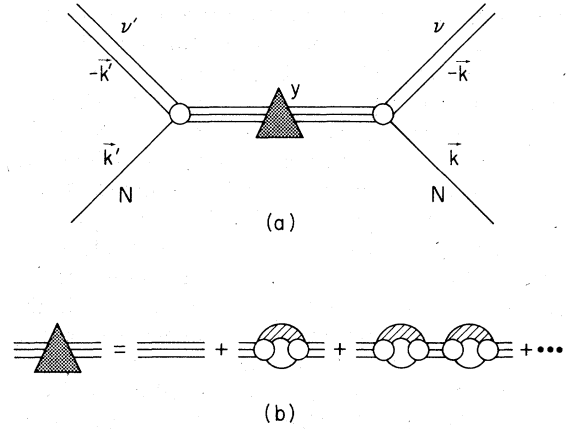


FIG. 3. (a) Graphical representation of the approximate amplitude for  $N\nu \rightarrow N\nu'$ .  $y$  is either  $t$ ,  $t'$ , or  $t''$  depending on the spin-isospin quantum numbers of the channel interaction. (b) First few terms in an expansion of the approximate three-particle propagator  $y$ .  $\nu$  and  $\nu'$  are either  $d$  or  $\phi$ .

formalism,

$$Z_t + s_{Nd} + s_{N\phi} = 1, \quad (9)$$

where  $Z_t$  is the probability of finding an elementary  $t$  in the wave function of the physical  $t$ , and  $s_{Nd}$  and  $s_{N\phi}$  are the spectroscopic factors for the  $N+d$  and  $N+\phi$  configuration, respectively. The relation between the spectroscopic factors and the parameters of the interaction is discussed in Appendix B.

Subject to these constraints the renormalized parameters of the interactions are adjusted to fit the most important three-body observables such as the triton binding energy ( $\epsilon_t = 8.48$  MeV), the nucleon+deuteron component of the triton wave function, and the doublet and quartet neutron-deuteron  $s$ -wave phase shifts and inelastic parameters. As in the work of Alt, Grassberger, and Sandhas,<sup>3</sup> the vertex functions  $g_{\nu y}(k)$  are chosen to have the same momentum dependence as the exact three-body Sturmian functions  $g_{\nu, i}^{UV}$  resulting from the solution of

$$g_{\nu, i}^{UV}(k; E) = [\eta_i^{UV}]^{-1} \sum_{\nu'=d, \phi} \int_0^\infty \frac{n^2 dn}{2\pi^2} \Lambda_{\nu\nu'}^{UV} \mathfrak{B}_{\nu\nu'}^i(k, n; E) \tau_{\nu'}(E + \epsilon_{\nu'} - \frac{3}{2}n^2) g_{\nu', i}^{UV}(n; E), \quad (10)$$

for  $l=0$  and corresponding to the largest eigenvalue  $\eta$ . It is well known<sup>3</sup> that for  $E < -\epsilon_d$  the largest eigenvalue solution of (10) can be represented with reasonable accuracy by an expression of the type

$$g(k; E) \Delta \{ [k^2 + \beta_1^2(E)][k^2 + \beta_2^2(E)][k^2 + \beta_3^2(E)] \}^{-1}, \quad (11)$$

where  $\beta_1, \beta_2, \beta_3$  depend on the three-body center-of-mass energy  $E$ . Therefore we adopt for  $g_{\nu y}(k)$  an expression that is identical to (11) but whose parameters  $\beta_1, \beta_2$ , and  $\beta_3$  are energy independent. For  $U=V=\frac{1}{2}$  the parameters of  $g_{\nu t}(k)$  ( $\nu=d$  or  $\phi$ ) are those that fit  $g_{\nu, i}^{UV}(k, E)$  at the three-body bound state energy.<sup>14</sup> The three-body coupling con-

stants  $\lambda_{\nu t}$  are chosen so that equal mixtures of  $N+d$  and  $N+\phi$  contribute to the three-nucleon wave function. This is a somewhat arbitrary procedure that can be justified by the approximate validity of the supermultiplet theory of Wigner<sup>15</sup> where the triplet and singlet nucleon-nucleon interactions are considered to be identical. For  $Z_t=0$  we have  $s_{Nd}=s_{N\phi}=0.5$ , where the  $s_{Nd}$  probability contains not only the nucleon+deuteron contribution but also the rescattering continuum of the triplet  $N-N$  interaction.<sup>16</sup> In the model, the resulting nucleon-deuteron component of the three-body bound state wave function is of the order of 40% which conforms with most predictions<sup>17</sup> including the one resulting from the exact solution of (10) with  $\eta=1$  and  $l=0$ . For the spin-isospin states  $(Q,D)$  and  $(D,Q)$  where there are no three-body bound states the parameters of  $g_{\nu y}(k)$  are taken to fit  $g_{\nu}^{UV0}(k,E)$  at the two-body scattering threshold  $E=-\epsilon_d$ , and the coupling constant  $\lambda_{\nu y}$  satisfies

$$\eta^{UV0} = \lambda_{\nu y}^2 \int \frac{d^3n}{(2\pi)^3} g_{\nu y}^2(k) \tau_{\nu}(E + \epsilon_{\nu} - \frac{3}{2}n^2), \quad (12)$$

at the same energy.

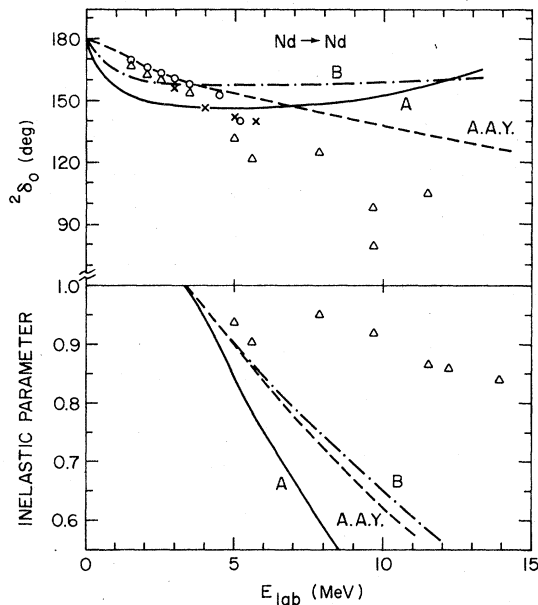


FIG. 4. Doublet phase shifts and inelastic parameters versus  $E_N$  resulting from the solution of Eq. (8) for  $Nd \rightarrow Nd$ . Curves A and B correspond to the two different sets of parameters in Table II. The open circles, the triangles, and the crosses result from the phase shift analyses of Refs. 18, 19 and 20, respectively. The dashed line corresponds to the solution of AAY equations (Ref. 13) with the two-body parameters of Appendix A and  $Z_d=0.051$ .

With the above choice of parameters the  $s$ -wave phase shifts  $^{2U+1}\delta_0$  and inelastic parameters resulting from the numerical solution of (8) for  $Nd$  elastic scattering are shown in Fig. 4 for  $U=\frac{1}{2}$  and in Fig. 5 for  $U=\frac{3}{2}$ . These results are compared with both AAY predictions and the most recent neutron-deuteron phase shift analyses. The values of the parameters are shown in Table II, where the sole purpose of set B for  $\beta_1$  and  $\lambda$  is to improve the fitting of the real part of the phase shifts to AAY three-body calculation. Both sets A and B are used to test the sensitivity of the four-body calculation to changes in the three-body amplitudes. Detailed numerical calculations have shown that in all three-body amplitudes where it is possible to define on-shell scattering, the inelastic parameter remains between 0 and 1 above breakup thresholds and returns to unity at sufficiently high energy. No gross violation of unitarity is observed in the three-body sector of our model and the 2-3 cross sections predicted by the optical theorem are non-negative. The total  $s$ -wave cross sections for elastic scattering and breakup are shown in Figs. 6 and 7 and are compared with AAY results.

We have therefore been able to formulate a one

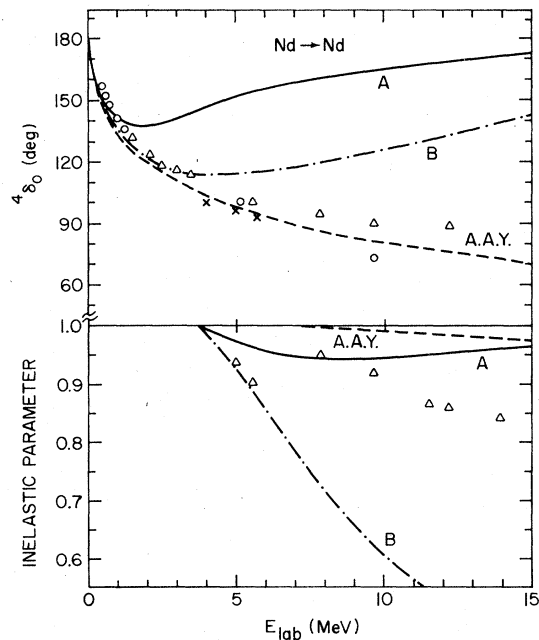


FIG. 5. Quartet phase shifts and inelastic parameters versus  $E_N$  resulting from the solution of Eq. (8) for  $Nd \rightarrow Nd$ . Curves A and B correspond to the two different sets of parameters in Table II. All other symbols are as in Fig. 4.

TABLE II. Parameter of the three-body  $T$  matrix in each spin-isospin channel interaction. Only  $\beta_1$  and  $\lambda$  have two sets of values, A and B.  $\beta_2$  and  $\beta_3$  are never changed. The units are ( $\text{fm}^{-1}$ ) for  $\beta$  and ( $\text{fm}^{-13}$ ) for  $\lambda^2$ .

		$t$		$t'$		$t''$	
		$U=\frac{1}{2}$ $Nd$	$V=\frac{1}{2}$ $N\phi$	$U=\frac{3}{2}$ $Nd$	$V=\frac{1}{2}$	$U=\frac{1}{2}$ $N\phi$	$V=\frac{3}{2}$
$\beta_1$	A	0.829	0.809	0.212		0.500	
	B	2.084	0.809	0.272		0.500	
$\beta_2$		2.075	2.473	1.936		2.404	
	$\beta_3$	3.706	2.867	2.923		2.441	
$\lambda$	A	270.8	-247.2	13.40		20.59	
	B	1257.0	-247.2	54.24		20.59	
$\epsilon$		8.48 MeV					
$Z$		0.0					

term separable representation of the three-body amplitude that has many features of the exact problem and whose parameters may be adjusted to the on-shell three-body data. At the expense of simplicity there is still room for considerable improvement. More separable terms per inde-

pendent amplitude can be easily allowed as well as vertex functions that are energy dependent and that become complex above scattering thresholds. In particular it may be appropriate to include the  $p$ -wave three-body amplitudes. They play an important role in neutron-deuteron scattering and as shown by Tjon<sup>4</sup> their presence affects the predictions of the four-body scattering calculation. Energy dependent three-body form factors are also required to correct for the absence of particle exchange diagrams at the three-body vertex. Since these two important features would

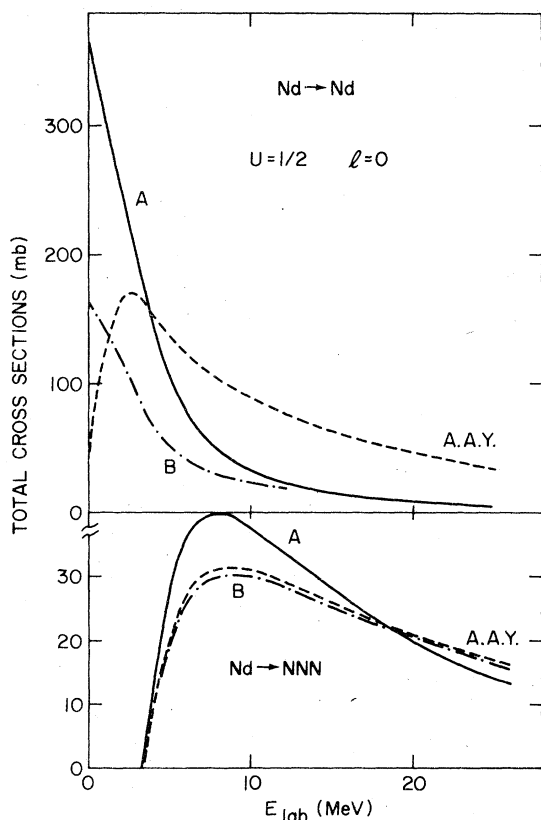


FIG. 6. Total doublet  $s$ -wave cross sections for  $Nd \rightarrow Nd$  and  $Nd \rightarrow NNN$  versus  $E_N$  resulting from the solution of Eq. (8). Curves A and B correspond to the two different sets of parameters in Table II. The dashed line corresponds to the solution of AAY equations (Ref. 13) with the two-body parameters of Appendix A and  $Z_d = 0.051$ .

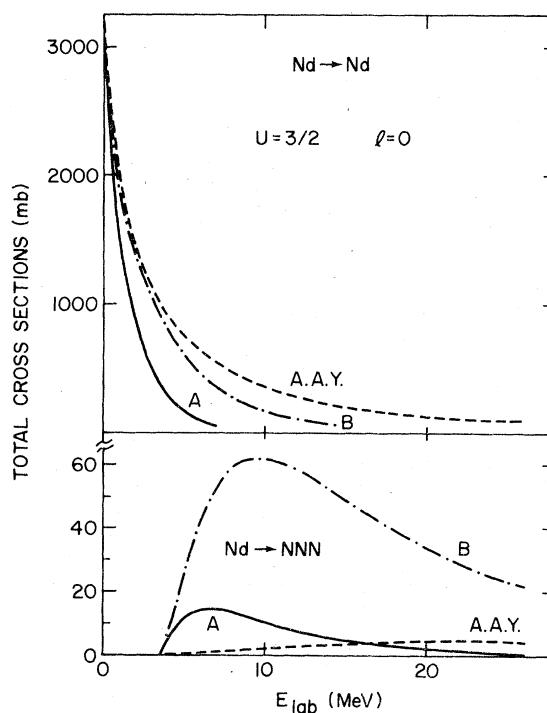


FIG. 7. Total quartet  $s$ -wave cross sections for  $Nd \rightarrow Nd$  and  $Nd \rightarrow NNN$  versus  $E_N$  resulting from the solution of Eq. (8). The notation is the same as in Fig. 6.

greatly increase the time involved in the numerical solution of the four-body equations shown below we postpone their inclusion for a subsequent publication where an improvement of the present model will be attempted.

### III. FOUR-BODY AMPLITUDES

Having introduced explicit fields coupled to  $N+d$  and  $N+\phi$  that led to three-body amplitudes in a separable form we now proceed to the four-body sector and consider all two-particle-to-two-particle amplitudes. The four-body equations that we obtain here are dynamically similar to the ones developed for four identical bosons<sup>11</sup> but some changes are necessary to account for the large number of  $1+3$  and  $2+2$  channels. The  $1+3$  channels to be considered are  $Nt$ ,  $Nt'$ , and  $Nt''$  while the  $2+2$  channels (named also quasiparticle-quasiparticle states) are  $dd$ ,  $d\phi$ , and  $\phi\phi$ .

As it has been previously pointed out the three-nucleon bound state  ${}^3\text{H}({}^3\text{He})$  is represented by a  $t$  with isospin projection  $+\frac{1}{2}$  ( $-\frac{1}{2}$ ) and likewise the  $N$  is either  $n$  or  $p$  depending on its isospin projection. Since in the model all short range interactions are charge independent and the long range Coulomb force has been disregarded, the results obtained from the solution of our equations for reactions initiated by charge symmetric states ( $p+{}^3\text{H}$  and  $n+{}^3\text{He}$  or  $p+{}^3\text{He}$  and  $n+{}^3\text{H}$ ) are identical. Therefore the two-to-two reactions of interest are  $n{}^3\text{He} \rightarrow n{}^3\text{He}$ ,  $n{}^3\text{He} \rightarrow p{}^3\text{H}$ , and  $n{}^3\text{He} \rightarrow dd$ ,  $n{}^3\text{H} \rightarrow n{}^3\text{H}$ , as well as  $dd \rightarrow dd$  and  $dd \rightarrow n{}^3\text{He}$ . As shown in Table III only the states  $n+{}^3\text{H}$ ,  $p+{}^3\text{H}$ , and  $d+d$  are pure states of the total isospin  $I$  with isospin projections  $I_z=1$ ,  $I_z=-1$ , and  $I_z=0$ , respectively. Both  $n+{}^3\text{He}$  and  $p+{}^3\text{H}$  have  $I_z=0$  but neither is a pure state of the total isospin. If we are to study the reactions initiated by  $n+{}^3\text{He}$  (or  $p+{}^3\text{H}$ ) the total  $I$  cannot be specified or otherwise the initial and final states become appropriate mixtures of  $n+{}^3\text{He}$  and  $p+{}^3\text{H}$ . In a preliminary study of our model we want to avoid unnecessary difficulties and for that reason we chose not to solve the equations for these particular reactions where the total isospin is not a good quantum number.<sup>21</sup> Instead we formulate and solve numerically the

TABLE III. Two-body reactions of interest.

$I_z \backslash I$	0	1	Mixed
-1		$p+{}^3\text{He}$	
0	$d+d$		$n+{}^3\text{He}; p+{}^3\text{H}$
1		$n+{}^3\text{H}$	

equations for the reactions initiated by  $n+{}^3\text{H}$  (or  $p+{}^3\text{He}$ ) and  $d+d$  for which the total  $I$  can be specified.

We want our four-body equations for the required processes to be of the Lippmann-Schwinger type where the kernel is given by the product of well-identified terms, that is, Born terms and intermediate propagators. As it has been discussed elsewhere<sup>22</sup> the presence of quasiparticle states as off-shell external lines make it difficult to separate the Born terms from the intermediate propagators. The four-body equations are therefore constructed in such a way that no quasiparticle-quasiparticle state ever appears as an off-shell external line. The simplifying assumptions adopted in the three-body sector of the model are carried through in the four-body sector, that is, virtual  $Nd$  or  $N\phi$  scattering can only occur in  $s$ -wave through the intermediate  $t$ 's. Therefore, in the absence of  $l>0$ ,  $Nd$  or  $N\phi$  scattering, the total four-body spin  $S$  and projection  $S_z$  are conserved. Concentrating first on the reactions initiated by the  $Nt$  state, a graphical representation of the integral equation for the  $Nt \rightarrow Ny$  ( $y=t, t'$ , or  $t''$ ) amplitude is illustrated in Fig. 8(a). In a representation in which  $S$ ,  $S_z$ ,  $I$ , and  $I_z$  are diagonal the equation reads

$$\langle \vec{k}' | \mathcal{T}_{yt}^{SI}(E) | \vec{k} \rangle = \langle \vec{k}' | g_{yt}^{SI}(E) | \vec{k} \rangle + \sum_{y''} \int \frac{d^3k''}{(2\pi)^3} \langle \vec{k}' | g_{yy''}^{SI}(E) | \vec{k}'' \rangle \times \tau_{y''}(E + \epsilon_{y''} - \frac{4}{3}k''^2) \times \langle \vec{k}'' | \mathcal{T}_{y''t}^{SI}(E) | \vec{k} \rangle, \quad (13)$$

where the  $y''$  summation runs over  $t, t'$  and  $t''$

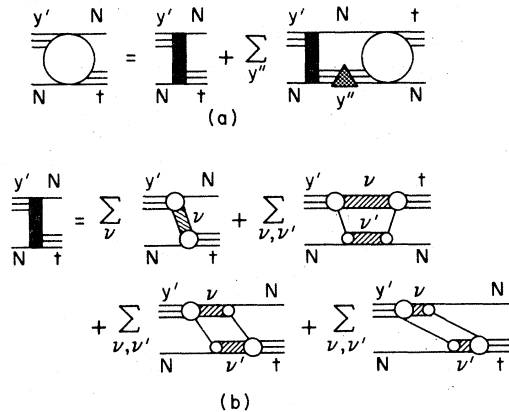


FIG. 8. Graphical representation of the integral equation for the  $Nt \rightarrow Ny'$  amplitude (circle).  $y'$  (or  $y''$ ) is  $t, t'$ , or  $t''$  and  $\nu$  (or  $\nu'$ ) is  $d$  or  $\phi$ .

and driving term  $g(E)$  is

$$g_{y,y}(E) = B_{y,y}(E) + \mathcal{E}_{y,y}(E) + \mathcal{X}_{y,y}(E). \quad (14)$$

$B_{y,y}(E)$  corresponds to the  $d$  or (and)  $\phi$  particle exchange Born term,  $\mathcal{E}_{y,y}(E)$  to the box amplitude depicted first in Fig. 8(b), and  $\mathcal{X}_{y,y}(E)$  to the sum of the last two box amplitudes. Both  $\mathcal{E}_{y,y}(E)$  and  $\mathcal{X}_{y,y}(E)$  may have as intermediate states the  $2+2$  channels  $dd$ ,  $d\phi$ ,  $\phi d$ , and  $\phi\phi$ . The Born term  $B_{y,y}(E)$  describes the exchange of two correlated and fully interacting particles while the box amplitudes involve the exchange of two uncorrelated particles in a two-step process. As shown in Table IV the number of two-body channels that contribute to (13) depends on  $S$  and  $I$ , and the number of coupled equations varies from one to a maximum of three. Since the  $dd$  channel is absent for an incoming  $n+^3\text{H}$  (or  $p+^3\text{He}$ ) state we need not write an equation for this particular rearrangement reaction.

For an incoming  $dd$  state we write the equations for both processes  $dd \rightarrow dd$  and  $dd \rightarrow n^3\text{He}$  (or  $p^3\text{He}$ ). As in a previous work<sup>11</sup> to avoid dealing with the quasiparticle-quasiparticle states as off-shell external lines we obtain first an integral equation for  $dd \rightarrow Ny$  ( $y = t, t'$  or  $t''$ ). The elastic amplitude  $dd \rightarrow dd$  is then calculated by performing an integration over the half-on-shell amplitude for  $dd \rightarrow Ny$ . The integral equation for  $dd \rightarrow Ny$  has been depicted in Fig. 9(a) and reads

$$\begin{aligned} \langle \vec{k}' | \mathcal{T}_{y dd}^{SI}(E) | \vec{k} \rangle &= \langle \vec{k}' | B_{y dd}^{SI}(E) | \vec{k} \rangle \\ &+ \sum_{y''} \int \frac{d^3 k''}{(2\pi)^3} \langle \vec{k}' | g_{y y''}^{SI}(E) | \vec{k}'' \rangle \\ &\times \tau_{y''}(E + \epsilon_{y''} - \frac{4}{3}k''^2) \\ &\times \langle \vec{k}'' | \mathcal{T}_{y'' dd}^{SI}(E) | \vec{k} \rangle. \end{aligned} \quad (15)$$

$B_{y dd}(E)$  is the single-particle exchange Born terms and  $g_{y y''}(E)$  is given by (14). The solution of this equation provides a means to obtain the elastic amplitude for  $dd \rightarrow dd$ . The precise form of the integral relation between  $\mathcal{T}_{y dd}$  and  $\mathcal{T}_{dd, dd}$  is

TABLE IV. Two-body channels in each spin-isospin interaction.

	$S=0$	$S=1$	$S=2$
$T=0$	$Nt$ $dd, \phi\phi$	$Nt, Nt'$ $dd$	$Nt'$ $dd$
$T=1$	$Nt, Nt''$ $\phi\phi$	$Nt, Nt', Nt''$ $d\phi$	$Nt'$
$T=2$	$Nt''$ $\phi\phi$	$Nt''$	

$$\begin{aligned} \langle \vec{k}' | \mathcal{T}_{dd, dd}^{SI}(E) | \vec{k} \rangle &= \sum_y \int \frac{d^3 k''}{(2\pi)^3} \langle \vec{k}' | B_{dd y}^{SI} | \vec{k}'' \rangle \\ &\times \tau_y(E + \epsilon_y - \frac{4}{3}k''^2) \\ &\times \langle \vec{k}'' | \mathcal{T}_{y dd}^{SI}(E) | \vec{k} \rangle, \end{aligned} \quad (16)$$

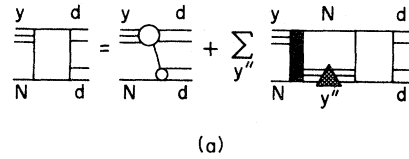
which is graphically represented in Fig. 9(b). Having written the equations for the required  $2+2$  amplitudes initiated by both  $n+^3\text{H}$  (or  $p+^3\text{He}$ ) and  $d+d$ , we now calculate the Born terms  $B_{y,y}(E)$  and  $B_{y dd}(E)$  as well as the box amplitudes  $\mathcal{E}_{y,y}(E)$  and  $\mathcal{X}_{y,y}(E)$ . The results are basically identical to the ones presented in Ref. 11, but more complicated due to the existence of spin and isospin quantum numbers. Although we have written Eqs. (13), (15), and (16) in a representation in which  $S$ ,  $S_z$ ,  $I$ , and  $I_z$  are diagonal, to carry out the explicit calculation of the Born terms and box amplitudes with the interaction Hamiltonians (1) and (7) it is most convenient to use a representation in which the spin and isospin projections of the individual particles are specified. The connection between the two representations has been left for Appendix C and indicate here just the final results. The two-particle exchange Born term  $B_{y,y}(E)$  can be written as

$$\langle \vec{k}' | B_{y y'}^{SI}(E) | \vec{k} \rangle = \sum_{\nu=d, \phi} \chi_{y y'}^{SI}(\vec{k}' | \bar{B}_{y y'}^{\nu}(E) | \vec{k}), \quad (17)$$

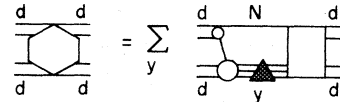
where

$$\begin{aligned} \langle \vec{k} | \bar{B}_{y y'}^{\nu}(E) | \vec{k} \rangle &= \lambda_{\nu y'} g_{\nu y'}(\vec{k} + \vec{k}'/3) \tau_{\nu}(X) \\ &\times \lambda_{\nu y} g_{\nu y}(\vec{k}' + \vec{k}/3), \end{aligned} \quad (18)$$

$$X = E + \epsilon_{\nu} - \vec{k}^2 - (\vec{k} + \vec{k}')^2/2 - \vec{k}'^2.$$



(a)



(b)

FIG. 9. (a) Graphical representation of the integral equation for the  $dd \rightarrow Ny$  amplitude (rectangle). (b) Graphical representation of the integral relation expressing the  $dd \rightarrow dd$  amplitude (hexagon) in terms of the half-on-shell  $dd \rightarrow Ny$  amplitude (rectangle).



The four-body spin-isospin recoupling coefficient  $\chi_{\nu y, y}^{SI}$  is given by

$$\chi_{\nu y, y}^{SI} = (-1)^{S+I+U+V-U'-V'} \hat{U} \hat{V} \hat{U}' \hat{V}' W(\frac{1}{2}, \Sigma, S, \frac{1}{2}; UU') \times W(\frac{1}{2}, \Theta, I, \frac{1}{2}; VV'), \quad (19)$$

where  $W$  is the Racah coefficient and  $\hat{U} = \sqrt{2U+1}$ .  $U-V$ ,  $U'-V'$ , and  $\Sigma-\theta$  are the spin-isospin quantum numbers of particles  $y$ ,  $y'$  and  $\nu$ , respectively. The single-particle exchange Born term  $B_{ydd}(E)$  is a special case of the more general Born term  $B_{y\nu\nu'}(E)$  ( $\nu, \nu' = d$  or  $\phi$ ) that may be written as

$$\langle \vec{k}' | B_{y\nu\nu'}^{SI}(E) | \vec{k} \rangle = (-1)^{\sqrt{2}} (1^{-\theta_{\nu\nu'}}) [\chi_{y\nu\nu'}^{SI} \langle \vec{k}' | \bar{B}_{y\nu\nu'}(E) | \vec{k} \rangle + (-1)^{S+I} \chi_{y\nu\nu'}^{SI} \langle \vec{k}' | \bar{B}_{y\nu\nu'}(E) | -\vec{k} \rangle], \quad (20)$$

where

$$\langle \vec{k}' | \bar{B}_{y\nu\nu'}(E) | \vec{k} \rangle = \frac{\gamma_{\nu'} f_{\nu'}(\vec{k}' + \frac{1}{2}\vec{k}) \lambda_{\nu y} g_{\nu y}(\vec{k} + \vec{k}'/2/3)}{E + \epsilon_{\nu} - \frac{1}{2}k^2 - (\vec{k} + \vec{k}')^2 - k'^2}, \quad (21)$$

and

$$\chi_{y\nu\nu'}^{SI} = \hat{U} \hat{V} \hat{\Sigma}' \hat{\Theta}' W(\frac{1}{2}, \frac{1}{2}, S, \Sigma; \Sigma' U) W(\frac{1}{2}, \frac{1}{2}, I, \Theta; \Theta' V). \quad (22)$$

$$G_1(E) = \tau_{\nu}(Y) \delta_{\nu d} - \frac{(Y-Q)(Y-Q')}{\pi} \int_0^{\infty} dx \frac{\text{Im}[\tau_{\nu}(x + \epsilon_{\nu})] \tau_{\nu'}(Y - \epsilon_{\nu} - x)}{(Y-Q - \epsilon_{\nu} - x)(Y-Q' - \epsilon_{\nu} - x)}, \quad (25)$$

and

$$G_2(E) = \frac{Y-Q''}{-Q''} \tau_{\nu}(Y) \delta_{\nu d} + \frac{(Y-Q)(Y-Q'')}{(Y-Q-Q'')} \tau_{\nu}(Q'') \tau_{\nu'}(Y-Q'') - \frac{(Y-Q)(Y-Q'')}{\pi} \int_0^{\infty} dx \frac{\text{Im}[\tau_{\nu}(x + \epsilon_{\nu})] \tau_{\nu'}(Y - \epsilon_{\nu} - x)}{(x + \epsilon_{\nu} - Q'')(Y-Q-Q' - \epsilon_{\nu} - x)}, \quad (26)$$

where

$$\begin{aligned} Y &= E + \epsilon_{\nu} + \epsilon_{\nu'} - k''^2, \\ Y-Q &= E + \epsilon_{\nu} - \frac{1}{2}k''^2 - (k+k'')^2 - k^2, \\ Y-Q' &= E + \epsilon_{\nu} - \frac{1}{2}k''^2 - (k'+k'')^2 - k'^2, \\ Y-Q'' &= E + \epsilon_{\nu} - \frac{1}{2}k''^2 - (k'-k'')^2 - k'^2. \end{aligned} \quad (27)$$

The Kronecker symbol  $\delta_{\nu d}$  makes the first term in both (25) and (26) equal to zero unless  $\nu = d$ . This terminates the description of the four-body equations for a system composed of four identical fermions. The structure of these equations is very similar to the four-body equations of Narodetskii<sup>8</sup> or Perne and Sandhas<sup>14</sup> for the same two-body  $N-N$  interaction, a single term in the Hilbert-Schmidt expansion of the  $1+3$  subamplitude, and all terms in the expansion of the  $2+2$  subampli-

ties. The box amplitudes  $\mathfrak{B}_{y\nu\nu'}(E)$  and  $\mathfrak{X}_{y\nu\nu'}(E)$  are constructed using the convolution procedure that has been discussed elsewhere.<sup>22</sup> We therefore present here just the final results,

$$\langle \vec{k}' | \mathfrak{B}_{y\nu\nu'}^{SI}(E) | \vec{k} \rangle = 2 \sum_{\nu\nu'} \int \frac{d^3k''}{(2\pi)^3} \chi_{y\nu\nu'}^{SI} \langle \vec{k}' | \bar{B}_{y\nu\nu'}(E) | \vec{k}'' \rangle \times G_1(E) \chi_{y\nu\nu'}^{SI} \langle \vec{k}'' | \bar{B}_{y\nu\nu'}(E) | \vec{k}'' \rangle, \quad (23)$$

and

$$\langle \vec{k}' | \mathfrak{X}_{y\nu\nu'}^{SI}(E) | \vec{k} \rangle = 2(-1)^{S+I} \times \sum_{\nu\nu'} \int \frac{d^3k''}{(2\pi)^3} \chi_{y\nu\nu'}^{SI} \langle \vec{k}' | \bar{B}_{y\nu\nu'}(E) | -\vec{k}'' \rangle \times G_2(E) \chi_{y\nu\nu'}^{SI} \langle \vec{k}'' | \bar{B}_{y\nu\nu'}(E) | \vec{k}'' \rangle, \quad (24)$$

where the summation in  $\nu$  and  $\nu'$  runs over both  $d$  and  $\phi$ . The  $G_1$  and  $G_2$  propagators are defined as

tudes. The main differences are the choice of three-body vertex functions and propagators to be used in the four-body sector and the treatment of the  $2+2$  subamplitudes. While in most other work a separable expansion of the  $1+3$  and  $2+2$  subamplitudes is required to reduce the four-body equations to one variable integral equations, in this work the  $2+2$  subamplitudes are treated exactly using the convolution method.<sup>22</sup> This seems to be a particularly convenient procedure in the scattering region where the correct treatment of all two-, three-, and four-body cuts is most needed.

#### IV. RESULTS

In this section we present the results obtained from the numerical solution of Eqs. (13), (15), and

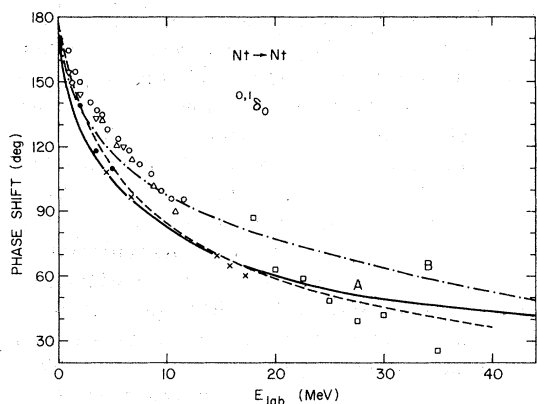


FIG. 10. Singlet  $s$ -wave phase shifts  ${}^{01}\delta_0$  versus  $E_N$ . Curves A and B correspond to the two different sets of parameters in Table II. The dashed line and the crosses correspond to the resonating-group calculation of Refs. 28 and 29, respectively. The black dots are the four-body results of Tjon (Ref. 4). All other data are from phase shift analyses: open circles from Ref. 24, inverse triangles from Ref. 25, triangles from Ref. 26, and squares from Ref. 27.

(16) for the reactions  ${}^3\text{He}(p,p){}^3\text{He}$ ,  ${}^3\text{H}(n,n){}^3\text{H}$ ,  ${}^2\text{H}(d,d){}^2\text{H}$ , and  ${}^2\text{H}(d,p){}^3\text{H}$ . Our integral equations contain one vector variable in intermediate states and reduce to single variable equations following partial wave decomposition. The singularity structure of the Born terms and box diagrams, though more complicated, is similar to that encountered in the three-body problem and the usual contour rotation method<sup>23</sup> together with matrix inversion has been used. The numerical calculations are straight-forward but lengthy mainly due to the convolution integrals used to obtain the box amplitudes. Using an 18 point integral equation mesh the CDC 7600 computer takes approximately three minutes to solve the equations for seven independent amplitudes in six partial waves (40 minutes for the IBM 370-158).

In Figs. 10 through 15 the  $Nt \rightarrow Nt$  phase shifts  ${}^{SI}\delta_l$  are shown for  $l=1$  and different values of  $S$  and  $l$ . Considering that the predictions of the

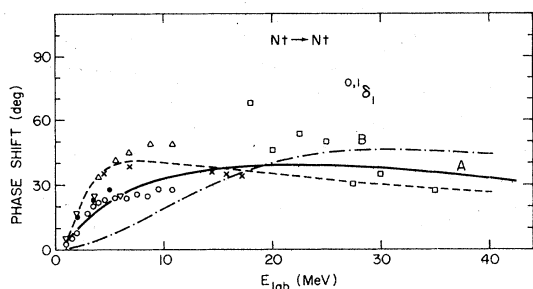


FIG. 11. Singlet  $p$ -wave phase shifts  ${}^{01}\delta_1$  versus  $E_N$ . All symbols are as in Fig. 10.

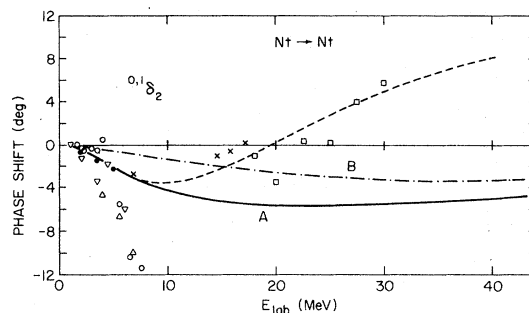


FIG. 12. Singlet  $d$ -wave phase shifts  ${}^{01}\delta_2$  versus  $E_N$ . All symbols are as in Fig. 10.

optical model or the  $R$ -matrix theory for the four-nucleon system are not on the basis of the two-nucleon interaction and involve some kind of preliminary fitting to chosen four-nucleon observables, we compare our results with the most recent phase shift analyses<sup>24-27</sup> and with the predictions of resonating-group calculations for  $p+{}^3\text{He}$  (Ref. 28) and  $n+{}^3\text{H}$ .<sup>29</sup> The corresponding phase shifts resulting from the four-body calculation of Tjon<sup>4</sup> are also displayed for comparison. The solid curves correspond to set A for the parameters  $\beta_1$  and  $\lambda$  of the three-body  $T$  matrix (see Table II) and the dash-dotted lines to set B. With the exception of  ${}^{11}\delta_1$  all other phase shifts conform with what is expected from previous calculations or phase shift analyses. The  $s$ -wave phase shifts are repulsive and satisfy the relation  ${}^{SI}\delta_0(E=0) - {}^{SI}\delta_0(E=\infty) = \pi$ . In the framework of the shell model the absence of positive parity  $l=1$  bound states in the four-nucleon system is attributed to the Pauli principle that prevents a third neutron (or proton) from occupying a position in an already filled  $s_{1/2}$  shell. Therefore the modified Levinson's theorem<sup>30</sup> may be invoked to justify

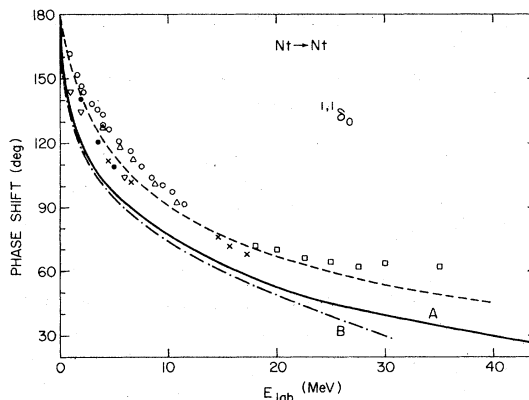


FIG. 13. Triplet  $s$ -wave phase shifts  ${}^{11}\delta_0$  versus  $E_N$ . All symbols are as in Fig. 10.

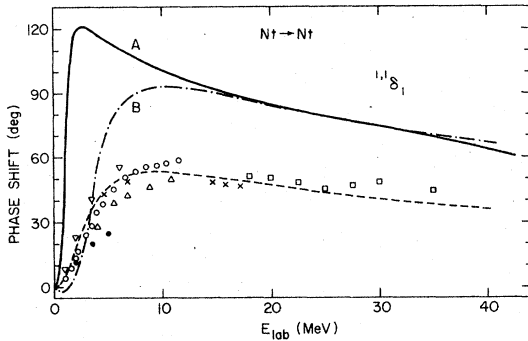


FIG. 14. Triplet  $p$ -wave phase shifts  $^{11}\delta_1$  versus  $E_N$ . All symbols are as in Fig. 10. The phase shifts of Refs. 24, 25, 26, and 27 had to be averaged over  $J$ .

the behavior of the  $s$ -wave  $n + {}^3\text{H}$  (or  $p + {}^3\text{He}$ ) phase shifts as due to the existence of a Pauli excluded  $l=0$  bound state. As in the phase shift analyses of Tombrello<sup>24</sup> the triplet  $s$ -wave phase shifts are smaller than those corresponding to the singlet state [if the  ${}^{51}\delta_0(E=0) = \pi$  convention is adopted] but they do not differ greatly in magnitude. The  $p$ -wave phase shifts exhibit the usual resonant structure. The singlet  $p$ -wave phase shifts resulting from set A seem to have the correct order of magnitude but the triplet  $^{11}\delta_1$  present a sharp rise through  $\pi/2$  that is not observed in any other calculation or phase shift analyses. With set B there is a slight improvement in  $^{11}\delta_1$  but the singlet phases become too small. The  $d$ -wave phase shifts are repulsive and, contrary to the prediction of the resonating-group calculations of Reichstein *et al.*<sup>28</sup> or the phase shift analyses of Morales *et al.*,<sup>27</sup> they do not change sign around  $E_p = 20$  MeV (proton laboratory energy). Since the resonating-group calculations do not take into account the effects of breakup and the phase shift analyses does not allow for complex phase shifts it is possible that our model calculation may give a better prediction that only an exact calculation can verify. The inelastic parameters are shown

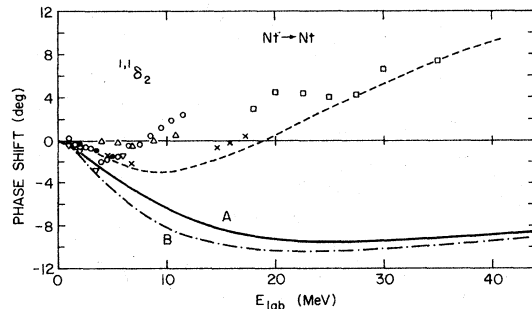


FIG. 15. Triplet  $d$ -wave phase shifts  $^{11}\delta_2$  versus  $E_N$ . All symbols are as in Fig. 10. The phase shifts of Refs. 26 and 27 had to be averaged over  $J$ .

in Fig. 16 for  $l=1, S=0, 1$ , and  $l=0, 1$ . In the absence of a rearrangement channel in  $l=1$ , inelasticity is due to three- and four-body breakup. The spin triplet interaction is more inelastic than the spin singlet. This may be attributed to the presence of  $d\phi$  states in  $S=1$  instead of  $\phi\phi$  states in  $S=0$  (see Table IV). While the  $d\phi$  boxes are responsible for three- and four-body inelasticity, the  $\phi\phi$  boxes only allow four-body intermediate states and for this reason are much less inelastic.

In Figs. 17–20 we show the differential cross sections for the isospin triplet  $Nt \rightarrow Nt$  elastic scattering process at energies between 1 and 30 MeV. The results of our calculation (curves A and B correspond to two different parametrizations of the three-body amplitudes—see Table II) are compared with experimental points from either  ${}^3\text{H}(n, n){}^3\text{H}$  or  ${}^3\text{He}(p, p){}^3\text{He}$  reactions. When comparing with  $p + {}^3\text{He}$  elastic data the Coulomb amplitude is added to the nuclear amplitudes multiplied by the appropriate Coulomb phases. Although our differential cross sections have the right shape and order of magnitude they do not fit the data equally well at all energies, particularly below 5 MeV. This is mainly due to the strong resonant behavior of the triplet  $p$ -wave phase shift at low energies. When set B is used and the resonance has broadened and moved to higher energies, there is a remarkable improvement particularly at 3.5 MeV where  $^{11}\delta_1$  has the order of magnitude that is expected by either phase shift analyses<sup>24–25</sup> or Tjon's calculation.<sup>4</sup> Above  $E_p = 6.5$  MeV our model calculation does quite well in reproducing the general trends of the experimental data. This is best seen in Fig. 21 where we plotted the total elastic cross section versus laboratory energy. Once again the sharp rise of the total cross section at

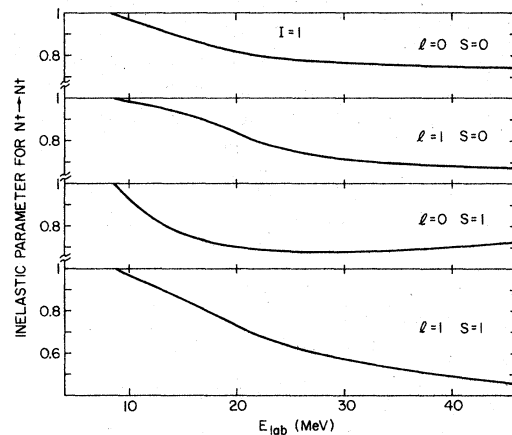


FIG. 16. Isospin triplet inelastic parameters versus  $E_N$ . The parameters of the three-body  $T$  matrix are from set A in Table II.

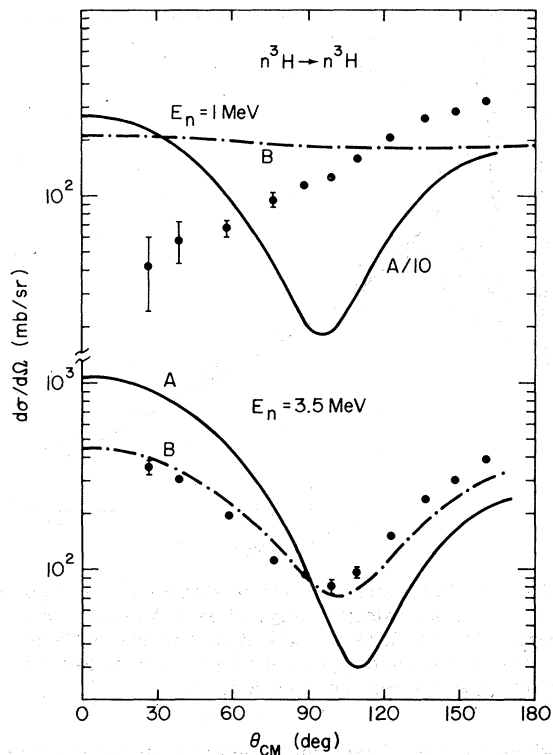


FIG. 17. Angular distribution for  ${}^3\text{H}(n, n){}^3\text{H}$  at different neutron laboratory energies. Curves A and B correspond to the two different sets of parameters in Table II. The black dots are experimental points from Ref. 31.

low energies is due to the triplet  $p$ -wave resonance. Above  $E_n = 6.5$  MeV the calculated cross section follows the experimental points and there is little difference between curve A and B. The total reaction cross section is shown in Fig. 22 and falls within the error bars of  $n + {}^3\text{H}$  data (crosses). Our calculation does not agree so well with the experimental reaction cross section for  $p + {}^3\text{He}$  (dots) but since Coulomb distortion can have an important effect on  $p + {}^3\text{He}$  results we do not consider this to be a serious discrepancy.

In Fig. 23 and 24 the differential cross sections for  $dd \rightarrow p{}^3\text{H}$  are shown for deuteron laboratory energies between 6.7 and 51.5 MeV. At low energies our differential cross sections lack sufficient structure but improve considerably at higher energies. Nevertheless the overall order of magnitude tends to be smaller than experiment. The elastic cross sections for  $dd \rightarrow dd$  are shown in Fig. 25 and although they have the correct shape the order of magnitude is much too small. Since  $nv$  ( $v = d$  or  $\phi$ ) scattering in the three-body sector of our model proceeds through an intermediate quasiparticle  $y$  ( $y = t, t'$  or  $t''$ ), there are many four-body diagrams (such as simultaneous exchange of two

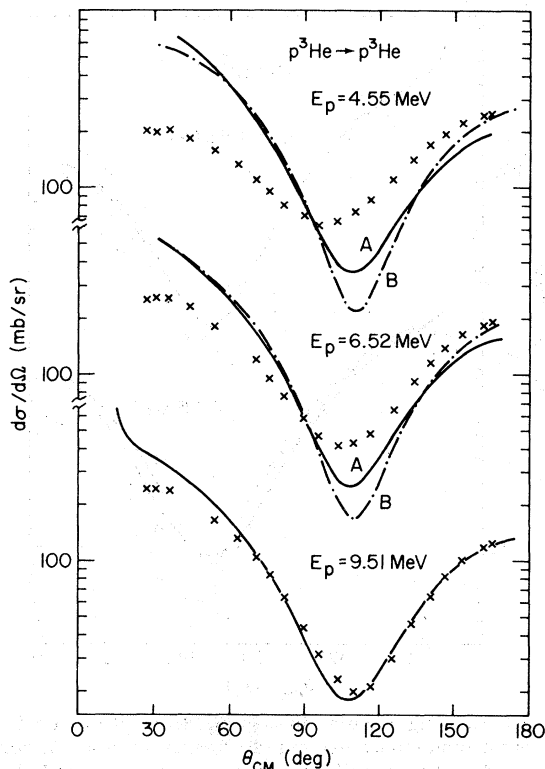


FIG. 18. Angular distribution for  ${}^3\text{He}(p, p){}^3\text{He}$  at different proton laboratory energies. The solid curves correspond to set A in Table II and the dash-dotted lines to set B. The crosses are experimental points from Ref. 32.

nucleons between two incoming deuterons) that are not allowed and whose contribution may be important to deuteron-deuteron elastic scattering (see Ref. 11). It is our hope that a better approximation to AAY three-body amplitudes would improve both the elastic and the rearrangement amplitudes.

## V. DISCUSSION

In the previous sections a four-nucleon model of the four-nucleon system was introduced and its numerical predictions compared with the appropriate experimental data. Two- and three-body scattering proceed through intermediate quasiparticles and the parameters of the interaction are fitted to the two- and three-nucleon observables (bound state and low energy scattering properties). The 2+2 subamplitudes are treated exactly by the convolution method and in this respect our approach differs from the work of Tjon,<sup>4</sup> Narodetskii,<sup>8</sup> or Perne and Sandhas.<sup>14</sup> In most of the previous work with nucleon-nucleon separable interactions a complete separable expansion of the 1+3 and 2+2 subamplitudes is required to

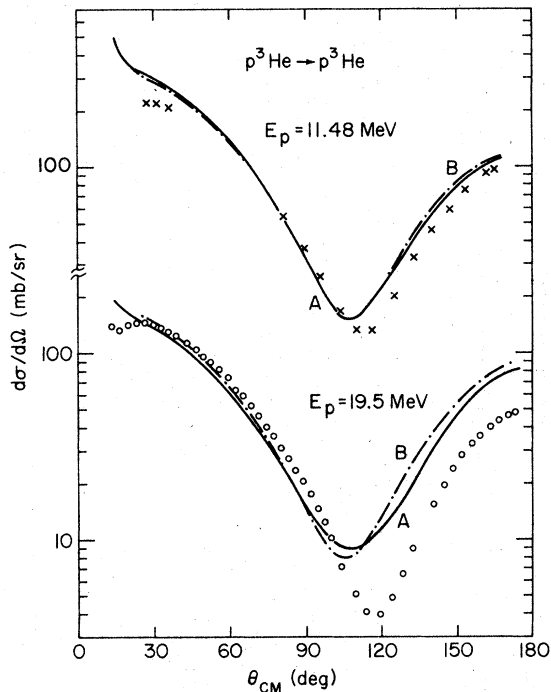


FIG. 19. Angular distribution for  ${}^3\text{He}(p,p){}^3\text{He}$  at different proton laboratory energies. Curves A and B correspond to the two different sets of parameters in Table II. The crosses are experimental points from Ref. 32 and the open circles are from Ref. 33.

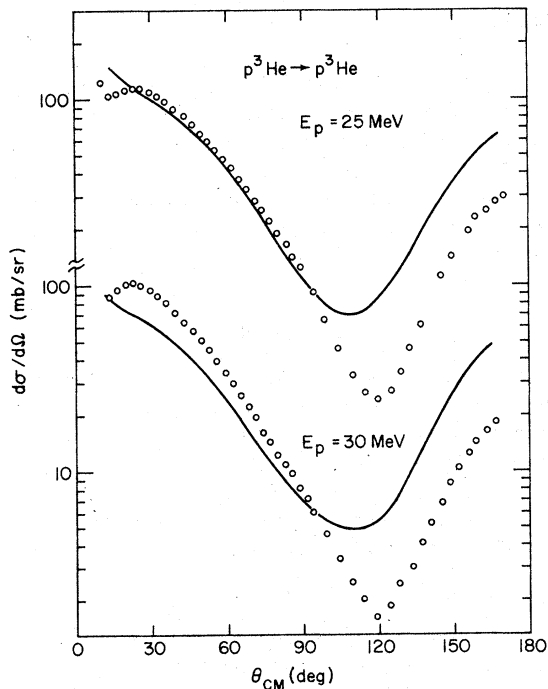


FIG. 20. Angular distribution for  ${}^3\text{He}(p,p){}^3\text{He}$  at different proton laboratory energies. The parameters are those from set A in Table II. The open circles are experimental points from Ref. 33.

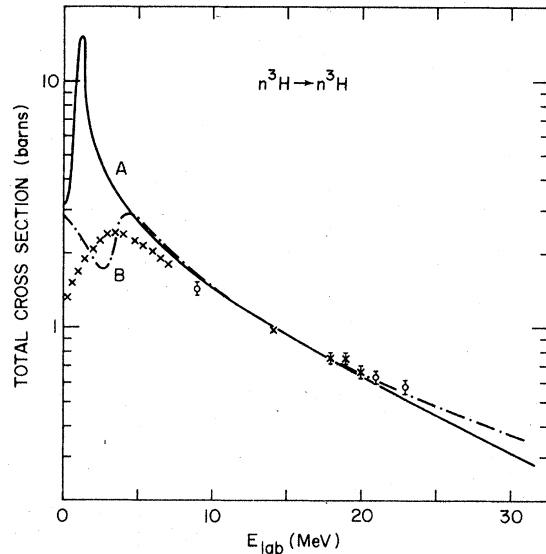


FIG. 21. Total elastic cross section for  $n{}^3\text{H} \rightarrow n{}^3\text{H}$  versus neutron laboratory energy. Curves A and B correspond to the two different sets of parameters in Table II. The crosses are experimental points from Ref. 34 and the open circles are from Ref. 35.

reduce the four-body equations to one vector variable in intermediate states. The method proposed here involves a one term separable representation of the 1+3 subamplitudes and the correct treatment of the 2+2 subamplitudes by the convolution method. As pointed out before we have adopted a very simple model three-body amplitude and there is plenty of room for further improvement. The next step would require choosing three-body vertex functions that are energy dependent and that become complex as the three-body center-of-mass energy increases beyond the first scattering threshold. The  $p$ -wave three-body amplitudes should also be included. It is our

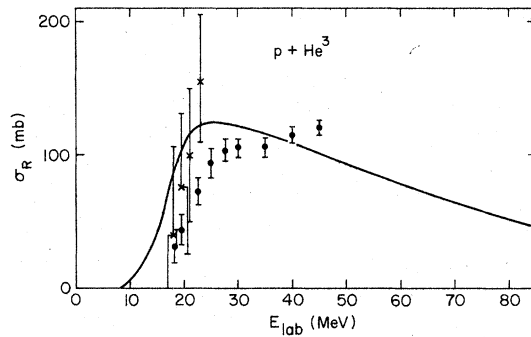


FIG. 22. Total reaction cross section for  $n+{}^3\text{He}$  neutron laboratory energy. The crosses are experimental points from Ref. 35. The black dots correspond to the experimental reaction cross section for  $p+{}^3\text{He}$  and are from Ref. 36.

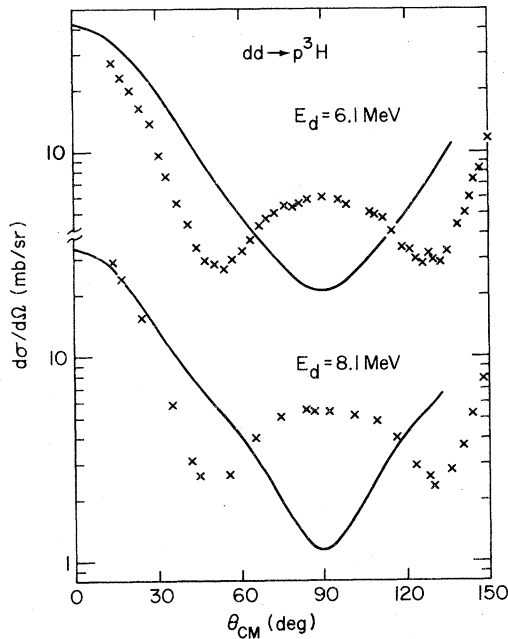


FIG. 23. Angular distribution for  ${}^2\text{H}(d,p){}^3\text{H}$  at different deuteron laboratory energies. The parameters of the three-body  $T$  matrix are from set A on Table II. The crosses are experimental points from Ref. 37.

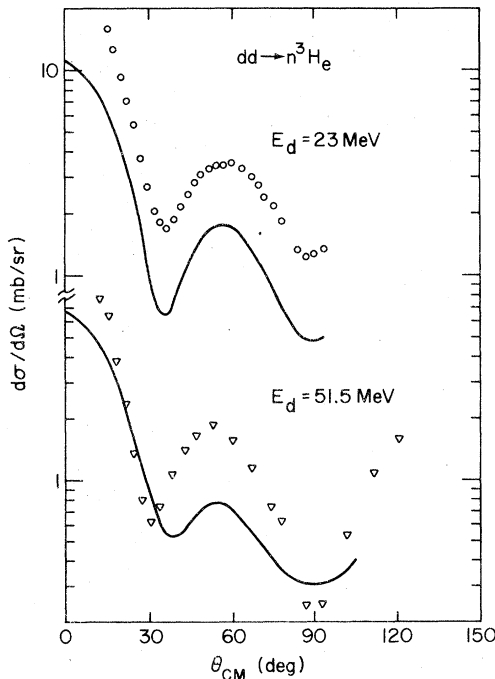


FIG. 24. Angular distribution for  ${}^2\text{H}(d,n){}^3\text{He}$  at different deuteron laboratory energies. The parameters of the three-body  $T$  matrix are from set A in Table II. The circles are experimental points from Ref. 38 and the inverted triangles from Ref. 39.

hope that such changes would greatly improve the results of our model, particularly in the low energy region where the amplitudes are more sensitive to the details of the three-body  $T$  matrix.

Since our four-body equations reduce to single variable integral equations after partial wave decomposition, and the singularity structure of the Born terms and box amplitudes is similar to that encountered in the three-body problem, the numerical techniques developed in the three-body problem were readily applied to the solution of these equations. With the present computer capabilities, our scattering equations are manageable within reasonable amounts of central processing unit (CPU) time and describe both qualitatively and quantitatively the main features of the four-nucleon scattering problem. The methods developed here can be easily applied to build four-body nuclear reaction models that can be solved in a computer with considerably less numerical effort than a more exact<sup>2</sup> formalism would allow. We are thinking in particular of nuclear reactions initiated by such states as  ${}^3\text{He} + \alpha$ ,  $p + {}^6\text{Li}$ , or  $\alpha + {}^6\text{Li}$  where, at low energies, the dominant reaction mechanism may be considered four-body. Since the energy required to break up an  $\alpha$ -particle is large compared to the energy of dissociation of  ${}^6\text{Li}$  into  $\alpha + n + p$  or  ${}^3\text{He}$  into  $p + d$  and  $p + n + d$ , one hopes that the internal degrees of freedom of the nucleons in the  $\alpha$  particle may be frozen and that such nuclear reactions may be well described as a four-body problem. Our approach

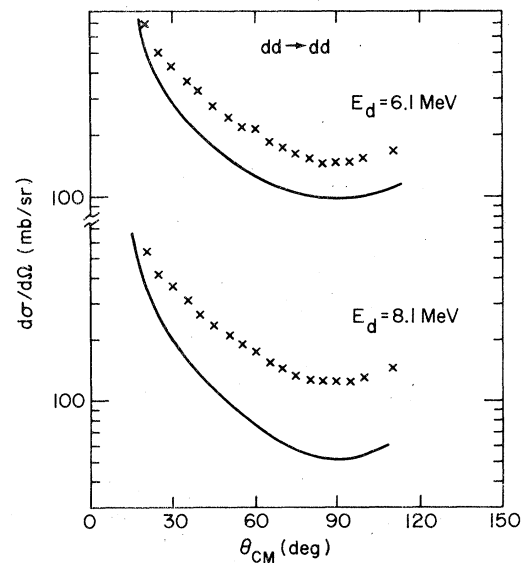


FIG. 25. Angular distribution for  ${}^2\text{H}(d,d){}^2\text{H}$  at different deuteron laboratory energies. The parameters of the three-body  $T$  matrix are from set A in Table II. The crosses are experimental points from Ref. 40.

has even the advantage that the breakup amplitudes can be easily expressed in terms of the two-to-two amplitudes<sup>22</sup> and are not much harder to calculate than the 2→3 amplitudes in the three-body problem. In a recent work<sup>42</sup> it has been shown that when the elementary constraints of unitarity and analyticity together with dispersion techniques are applied to three- and four-body final states in the quasiparticle isobar picture, a set of integral equations for the few-body amplitudes is obtained that is very similar to ours. Therefore it is our hope that the four-body formalism previously described exhibits enough features of the experimental problem to provide a good description of four-body scattering processes.

The author wishes to thank P. E. Shanley for useful discussions and the Computer Science Center of the University of Maryland for their generous collaboration. This work was supported by the U. S. Department of Energy.

#### APPENDIX A: TWO-PARTICLE PROPAGATORS: $\tau_d, \tau_\phi$

(1)  $\tau_d(E)$ : As it has been previously pointed out,  $N$ - $N$  scattering proceeds through the  $d$  each time a spin triplet pair interacts. Since the triplet interaction is responsible for the two-nucleon bound state, the  $\tau_d$  propagator is constructed by summing a series of self-energy bubbles [see Fig. 1(b)] and is renormalized so that a pole appears at the deuteron binding energy. For the vertex function we chose the Hulthen form  $f(\vec{n}) = (\vec{n}^2 + \beta_d^2)^{-1}$  and for that reason, the expressions that describe  $\tau_d$  are the same as in AAY,<sup>13</sup>

$$\tau_d(X) = \frac{S_d(X)}{X}, \quad (A1)$$

$$[S_d(X)]^{-1} = Z_d + \frac{\gamma_d^2}{16\pi} \zeta. \quad (A2)$$

For  $\alpha_d = \sqrt{\frac{1}{2}\epsilon_d}$  and  $\sigma = (X - \epsilon_d) < 0$ ,  $\zeta$  is real and is given by

$$\zeta = [2\beta_d(\alpha_d + \beta_d)(\alpha_d + \sqrt{-\frac{1}{2}\sigma})(\beta_d + \sqrt{-\frac{1}{2}\sigma})^{-1} \times [(\alpha_d + \beta_d)^{-1} + (\beta_d + \sqrt{-\frac{1}{2}\sigma})^{-1}], \quad (A3)$$

whereas for  $\sigma = (X - \epsilon_d) > 0$ ,  $\zeta$  is complex and is

$$\begin{aligned} \text{Re}\zeta &= 4[(\alpha_d + \beta_d)(2\beta_d^2 + \sigma)(\epsilon_d + \sigma)]^{-1} \\ &\times \left[ \frac{2\alpha_d\beta_d - \sigma}{2\beta_d^2 + \sigma} - \frac{\sigma + \epsilon_d}{4\beta_d(\alpha_d + \beta_d)} \right], \\ \text{Im}\zeta &= \sqrt{2\sigma}[(\epsilon_d + \sigma)(\beta_d^2 + \frac{1}{2}\sigma)^2]^{-1}. \end{aligned} \quad (A4)$$

The coupling constant  $\gamma_d$  can also be written as

$$\gamma_d^2 = 32\pi\alpha_d\beta_d(\alpha_d + \beta_d)^3(1 - Z_d). \quad (A5)$$

The triplet interaction is therefore characterized by the binding energy of the deuteron  $\epsilon_d$ , by the range parameter of the vertex functions  $\beta_d$ , and by the wave function renormalization constant  $Z_d$ . In terms of the low energy parameters of the triplet nucleon-nucleon interaction we have

$$\frac{1}{\alpha_d} = \frac{\alpha_d\beta_d^3 Z_d}{2(\beta_d + \alpha_d)^3(1 - Z_d)} + \frac{\alpha_d\beta_d(2\beta_d + \alpha_d)}{2(\beta_d + \alpha_d)^2}, \quad (A6)$$

and

$$\alpha_d = \sqrt{\frac{1}{2}\epsilon_d}, \quad (A7)$$

where  $a_d$  is the triplet scattering length. For  $\epsilon_d = 2.226$  MeV,  $\alpha_d = 5.41$  fm, and  $Z_d = 0$ ,  $\beta_d$  is obtained through (A6) and  $\gamma_d$  with the help of (A5).

(2)  $\tau_\phi(E)$ : The singlet nucleon-nucleon interaction is attractive but not strong enough to produce a bound state of the two-nucleon system. In the model the singlet interaction is characterized by the unphysical quasiparticle  $\phi$  whose propagator is constructed as in AAY (Ref. 13) and is given by

$$\tau_\phi(E) = - \left[ 1 + \gamma_\phi^2 \int \frac{d^3n}{(2\pi)^3} \frac{f_\phi^2(n)}{E - 2\vec{n}^2} \right]^{-1}. \quad (A8)$$

For a vertex function of the Hulthen shape the integral in the denominator of (A8) can be easily performed. For  $E < 0$ ,

$$\tau_\phi(E) = (-) \left[ 1 - \frac{\gamma_\phi^2}{16\pi} \frac{1}{\beta_\phi} \frac{1}{(\beta_\phi + \sqrt{-\frac{1}{2}E})^2} \right]^{-1}, \quad (A9)$$

while for  $E > 0$

$$\tau_\phi(E) = (-) \left[ 1 - \frac{\gamma_\phi^2}{16\pi} \frac{1}{\beta_\phi} \frac{1}{(\beta_\phi - i\sqrt{\frac{1}{2}E})^2} \right]^{-1}. \quad (A10)$$

In terms of the low energy parameters of the singlet nucleon-nucleon interaction we have

$$\beta_\phi = \frac{3}{2r_\phi} \left[ 1 + \left( 1 - \frac{16r_\phi}{9a_\phi} \right)^{1/2} \right], \quad (A11)$$

and

$$\gamma_\phi^2 = \frac{16\pi\beta_\phi^4 a_\phi}{\alpha_\phi\beta_\phi - 2}, \quad (A12)$$

where  $a_\phi$  and  $r_\phi$  are the singlet scattering length and effective range, respectively. For  $a_\phi = -23.78$  fm and  $r_\phi = 2.67$  fm the two parameters  $\beta_\phi$  and  $\gamma_\phi$  that characterize the singlet  $N$ - $N$  interaction in the model are determined through (A11) and (A12).

APPENDIX B: THREE-PARTICLE PROPAGATORS:  $\tau_t, \tau_{t'}, \tau_{t''}$ 

(1)  $\tau_t(E)$ : Since the  $t$  quasiparticle is coupled to both  $N+d$  and  $N+\phi$ , the  $t$  propagator is constructed by summing a series of  $Nd$  and  $N\phi$  bubbles. The propagator is graphically shown in Fig. 3(b) and the corresponding unrenormalized amplitude is given by

$$\tau_t^{(u)} = \frac{1}{E + \epsilon_t^{(0)}} + \frac{1}{E + \epsilon_t^{(0)}} I(E) \frac{1}{E + \epsilon_t^{(0)}} + \dots, \quad (\text{B1})$$

where  $-\epsilon_t^{(0)}$  is the bare energy of the  $t$  at rest.  $I(E)$  may be written as

$$I(E) = (\lambda_{dt}^{(u)})^2 \int \frac{d^3n}{(2\pi)^3} g_{dt}^2(n) \tau_d^{(u)}(E + \epsilon_d - \frac{3}{2}\hbar^2) + (\lambda_{\phi t}^{(u)})^2 \int \frac{d^3n}{(2\pi)^3} g_{\phi t}^2(n) \tau_\phi^{(u)}(E - \frac{3}{2}\hbar^2) \quad (\text{B2})$$

and represents the sum of two bubbles, one involving an  $N$  and a fully dressed  $d$  and the other an  $N$  and a fully dressed  $\phi$ . The  $d$  and  $\phi$  particle propagators are taken to be unrenormalized. Summing (B1) we have

$$(\tau_t^{(u)})^{-1} = E + \epsilon_t^{(0)} - I(E). \quad (\text{B3})$$

Requiring that  $\tau_t^{(u)}$  have a pole at the triton binding energy  $E = -\epsilon_t$  gives the relation

$$\epsilon_t^{(0)} = \epsilon_t + I(-\epsilon_t). \quad (\text{B4})$$

Assigning to the renormalized propagator  $\tau_t = \tau_t^{(u)}/Z_t$  a unit residue at the pole we obtain

$$\tau_t(X) = S_t(X)/X, \quad (\text{B5})$$

$$[S_t(X)]^{-1} = Z_t - \frac{\lambda_{dt}^2}{X} \int \frac{d^3n}{(2\pi)^3} g_{dt}^2(n) \times [\tau_d(X+Y) - \tau_d(Y)] - \frac{\lambda_{\phi t}^2}{X} \int \frac{d^3n}{(2\pi)^3} g_{\phi t}^2(n) \times [\tau_\phi(X+W) - \tau_\phi(W)], \quad (\text{B6})$$

$$X = E + \epsilon_t,$$

$$Y = \epsilon_d - \epsilon_t - \frac{3}{2}\hbar^2,$$

$$W = -\epsilon_t - \frac{3}{2}\hbar^2,$$

where the renormalized coupling constants are given by

$$\lambda_{\nu t} = \sqrt{Z_\nu Z_t} \lambda_{\nu t}^{(u)}, \quad (\text{B7})$$

and  $\tau_\nu = \tau_\nu^{(u)}/Z_\nu$ . The wave function renormalization constant  $Z_t$  is such that

$$Z_t + s_{Nd} + s_{N\phi} = 1, \quad (\text{B8})$$

where

$$s_{Nd} = \lambda_{dt}^2 \int \frac{d^3n}{(2\pi)^3} g_{dt}^2(n) \tau_d'(Y), \quad (\text{B9})$$

and

$$s_{N\phi} = \lambda_{\phi t}^2 \int \frac{d^3n}{(2\pi)^3} g_{\phi t}^2(n) \tau_\phi'(W). \quad (\text{B10})$$

$\tau_d'$  and  $\tau_\phi'$  are the derivatives of  $\tau_d$  and  $\tau_\phi$ , respectively, and  $s_{Nd}$  and  $s_{N\phi}$  are the spectroscopic factor for the  $N+d$  and  $N+\phi$  configurations. The spin  $\frac{1}{2}$ , isospin  $\frac{1}{2}$  three-body  $s$ -wave amplitude is therefore characterized by  $\epsilon_t$ ,  $g_{dt}$ , and  $g_{\phi t}$  in addition to  $Z_t$ ,  $s_{Nd}$ , and  $s_{N\phi}$ . In all calculations  $Z_t = 0$  and  $s_{Nd} = s_{N\phi} = 0.5$ .

(2)  $\tau_{t'}(E)$ : The  $t'$  quasiparticle is meant to approximate the spin quartet  $l=0$  state of the three-nucleon interaction. In the model,  $Nd$  scattering proceeds through the  $t'$  each time an  $N$  and a  $d$  interact in a state of total spin  $\frac{3}{2}$  and total isospin  $\frac{1}{2}$ . Since the spin quartet interaction is repulsive there is no bound state of the three-nucleon system with such quantum numbers, and the  $t'$  is an unstable particle with no physical analog. We construct the unrenormalized propagator  $\tau_{t'}^{(u)}$  by summing a series of  $Nd$  bubbles such that

$$(\tau_{t'}^{(u)})^{-1} = E + \epsilon_{t'}^{(0)} - (\lambda_{dt'}^{(u)})^2 \times \int \frac{d^3n}{(2\pi)^3} g_{dt'}^2(n) \tau_d^{(u)}(E + \epsilon_d - \frac{3}{2}\hbar^2). \quad (\text{B11})$$

The renormalization method for unstable quasiparticles has been developed elsewhere<sup>41</sup> so as to give the renormalized propagator  $\tau_{t'} = \tau_{t'}^{(u)}/Z_{t'}$ , the form it would have if a separable potential was used between the two interacting particles. Since the  $t'$  is an unstable particle,  $Z_{t'}$  is necessarily zero and in that limit we obtain

$$[\tau_{t'}(E)]^{-1} = 1 - \lambda_{dt'}^2 \times \int \frac{d^3n}{(2\pi)^3} g_{dt'}^2(n) \tau_d(E + \epsilon_d - \frac{3}{2}\hbar^2) \quad (\text{B12})$$

by taking

$$\lim_{Z_{t'} \rightarrow 0} Z_{t'} \epsilon_{t'}^{(0)} = 1, \quad (\text{B13})$$

and

$$\lim_{Z_{t'} \rightarrow 0} \sqrt{Z_d Z_{t'}} \lambda_{dt'}^{(u)} = \lambda_{dt'}. \quad (\text{B14})$$



Apart from the  $d$  bubbles that are expressed through  $\tau_d$ , the  $\tau_t$  is the same one would obtain if a repulsive separable potential was used between  $N$  and  $d$ . In the model, the spin quartet interaction is therefore characterized by the coupling constant  $\lambda_{dt'}$ , and the vertex function  $g_{dt'}$ .

(3)  $\tau_{t''}(E)$ : For the  $t''$  propagator we proceed as for the  $t'$  propagator and sum a series of  $N\phi$  bubbles. Using an identical renormalization procedure we obtain

$$[\tau_{t''}(E)]^{-1} = 1 - \lambda_{\phi t''}{}^2 \times \int \frac{d^3n}{(2\pi)^3} g_{\phi t''}{}^2(n) \tau_{\phi}(E - \frac{3}{2}n^2). \quad (\text{B15})$$

In the model the isospin quartet interaction is therefore characterized by the coupling constant  $\lambda_{\phi t''}$  and the vertex function  $g_{\phi t''}$ .

### APPENDIX C: SPIN AND ISOSPIN FACTORS

The solution of the four-body integral equations as described in Sec. III is most easily done in a representation in which the spin and the isospin of the channel are diagonal. On the contrary to calculate the Born terms and box amplitudes it is most convenient to use a representation in which the spin and isospin projections of the individual particles are specified. It is therefore necessary to relate both representations, and as an example of the procedure we will write the necessary relations for the two-particle exchange Born term  $B_{y'y}(E)$ .

In the representation in which the spin and isospin projections are specified the Born term  $B_{y'y}(E)$  may be written as

$$\langle U', u'; V', v'; \frac{1}{2}, s'; \frac{1}{2}, i'; \vec{k}' | B_{y'y}(E) | U, u; V, v; \frac{1}{2}, s; \frac{1}{2}, i; \vec{k} \rangle = \sum_{\substack{\Sigma, \sigma \\ \Theta, \theta}} (-1)^{\langle \vec{k}' | \bar{B}_{y'y}(E) | \vec{k} \rangle \langle \frac{1}{2}, \Sigma, s', \sigma | U, u \rangle} \times \langle \frac{1}{2}, \Sigma, s, \sigma | U', u' \rangle \langle \frac{1}{2}, \Theta, i', \theta | V, v \rangle \langle \frac{1}{2}, \Theta, i, \theta | V', v' \rangle, \quad (\text{C1})$$

where  $\langle \vec{k}' | \bar{B}_{y'y}(E) | \vec{k} \rangle$  is given by (18), and  $s$  and  $i$  are the spin and isospin projections of the nucleon. In terms of the spin and isospin of the channel

$$\langle \vec{k}' | B_{y'y}^{SI}(E) | \vec{k} \rangle \sum_{\substack{u, s, u', s' \\ v, i, v', i'}} \langle \frac{1}{2}, U, s, u | S, S_z \rangle \langle \frac{1}{2}, U', s', u' | S, S_z \rangle \langle \frac{1}{2}, V, i, v | I, I_z \rangle \times \langle \frac{1}{2}, V', i', v' | I, I_z \rangle \langle U', u'; V', v'; \frac{1}{2}, s'; \frac{1}{2}, i'; \vec{k}' | B_{y'y}(E) | U, u; V, v; \frac{1}{2}, s; \frac{1}{2}, i; \vec{k} \rangle. \quad (\text{C2})$$

Substituting (C1) in (C2) we obtain (17) after reducing the Clebsch-Gordan coefficients.

<sup>1</sup>L. D. Faddeev, Zh. Eksp. Teor. Fiz. 39, 1459 (1960) [Sov. Phys.—JETP, 12, 1014 (1961)]; Dokl. Akad. Nauk SSSR 138, 565 (1961) [Sov. Phys. Doklady 6, 384 (1961)]; 145, 301 (1967) [Z., 60 (1963)].

<sup>2</sup>O. A. Yakubovskii, Yad. Fiz. 5, 1312 (1967) [Sov. J. Nucl. Phys. 5, 937 (1967)]; P. Grassberger and W. Sandhas, Nucl. Phys. B2, 181 (1967); I. Sloan, Phys. Rev. C 6, 1945 (1972); G. Bencze, Nucl. Phys. A210, 568 (1973); E. F. Redish, *ibid.* A225, 16 (1974); W. Tobocman, Phys. Rev. C 9, 2466 (1974); D. J. Kouri and F. S. Levin, Nucl. Phys. A253, 395 (1975).

<sup>3</sup>E. O. Alt, P. Grassberger, and W. Sandhas, Phys. Rev. C 1, 85 (1970); M. Sawicki and J. M. Namyslowski, Phys. Lett. 60B, 331 (1976).

<sup>4</sup>J. A. Tjon, Phys. Lett. 63B, 391 (1976).

<sup>5</sup>H. Kröger and W. Sandhas, Phys. Rev. Lett. 40, 834 (1978).

<sup>6</sup>Kröger and Sandhas (Ref. 5) have reported 10 h. of Central processing unit time in the IBM 370/168 to obtain a set of four phase shifts at a given energy below rearrangement and breakup thresholds. The bound state calculation of B. F. Gibson and D. R. Lehman (Ref. 7) take approximately two minutes on the CDC 7600 computer.

<sup>7</sup>B. F. Gibson and D. R. Lehman, Phys. Rev. C 14, 685

(1976).

<sup>8</sup>I. M. Narodetskii, E. S. Galpern, and V. N. Lyakhovitsky, Phys. Lett. 46B, 51 (1973); I. M. Narodetskii, Nucl. Phys. A221, 191 (1974).

<sup>9</sup>J. A. Tjon, Phys. Lett. 56B, 217 (1975); Phys. Rev. Lett. 40, 1239 (1978).

<sup>10</sup>V. F. Karchenko and V. P. Levashev, Phys. Lett. 60B, 317 (1976).

<sup>11</sup>A. C. Fonseca and P. E. Shanley, Phys. Rev. C 14, 1343 (1976).

<sup>12</sup>R. D. Amado, Phys. Rev. 132, 485 (1963).

<sup>13</sup>R. Aaron, R. D. Amado, and Y. Y. Yam, Phys. Rev. 140, B1291 (1965).

<sup>14</sup>R. Perne and W. Sandhas, Phys. Rev. Lett. 39, 788 (1977).

<sup>15</sup>E. P. Wigner, Phys. Rev. 51, 106 (1937).

<sup>16</sup>See Appendix B for further discussion.

<sup>17</sup>Y. E. Kim and A. Tubis, Annu. Rev. Nucl. Sci. 24, 69 (1974).

<sup>18</sup>R. S. Christian and J. L. Gammel, Phys. Rev. 91, 100 (1953).

<sup>19</sup>W. T. H. Van Oers and K. W. Brockman, Nucl. Phys. A92, 561 (1967).

<sup>20</sup>P. A. Schmelzbach, W. Grüebler, R. E. White, V. König, R. Ritsler, and P. Marmier, Nucl. Phys.

- A197, 273 (1972).
- <sup>21</sup>They involve a larger number of four-body coupled equations.
- <sup>22</sup>A. C. Fonseca and P. E. Shanley, Phys. Rev. D 13, 2255 (1976).
- <sup>23</sup>J. H. Hetherington and L. H. Schick, Phys. Rev. 137, B935 (1965).
- <sup>24</sup>T. A. Tombrello, Phys. Rev. 138, B40 (1965).
- <sup>25</sup>T. A. Tombrello, Phys. Rev. 143, 772 (1966).
- <sup>26</sup>D. H. McSherry and S. D. Baker, Phys. Rev. C 1, 888 (1970).
- <sup>27</sup>J. R. Morales, T. A. Cahill, and D. J. Shadoan, Phys. Rev. C 11, 1905 (1975).
- <sup>28</sup>I. Reichstein, D. R. Thompson, and Y. C. Tang, Phys. Rev. C 3, 2139 (1971).
- <sup>29</sup>M. LeMere, R. E. Brown, Y. C. Tang, and D. R. Thompson, Phys. Rev. C 12, 1140 (1975).
- <sup>30</sup>P. Swan, Proc. R. Soc. London 228, 10 (1955); Ann. Phys. (N.Y.) 48, 10 (1968); A. Temkin, J. Math. Phys. 2, 336 (1961).
- <sup>31</sup>J. D. Seagrave, L. Cranberg, and J. E. Simmons, Phys. Rev. 119, 1981 (1960).
- <sup>32</sup>T. B. Clegg, A. C. L. Barnard, J. B. Swint, and J. L. Weil, Nucl. Phys. 50, 621 (1964).
- <sup>33</sup>R. E. Brown, B. T. Murdoch, D.K. Hasell, A. M. Sourkes, and W. T. H. Van Oers, in *Few Body Systems and Nuclear Forces*, proceedings of the VIII International Conference on Few Body Systems and Nuclear Forces, 1978, Graz, Austria, edited by H. Zingl, M. Haftel, and H. Zankel (Springer, Berlin, 1978), Vol. I, p. 292.
- <sup>34</sup>Los Alamos Physics and Cryogenics Groups, Nucl. Phys. 12, 291 (1959).
- <sup>35</sup>J. D. Seagrave *et al.*, Ann. Phys. (N.Y.) 74, 250 (1972).
- <sup>36</sup>A. M. Sourkes, A. Houdayer, and W. T. H. Van Oers, Phys. Rev. C 13, 451 (1976).
- <sup>37</sup>J. E. Brolley, T. M. Putnam, and L. Rosen, Phys. Rev. 107, 820 (1957).
- <sup>38</sup>W. T. H. Van Oers and K. W. Brockman, Nucl. Phys. 48, 625 (1963).
- <sup>39</sup>H. Brückmann, E. L. Haase, W. Kluge, and L. Schänzler, Z. Phys. 230, 383 (1970).
- <sup>40</sup>A. S. Wilson, M. C. Taylor, J. C. Legg and G. C. Phillips, Nucl. Phys. A126, 193 (1969).
- <sup>41</sup>M. T. Vaughn, R. Aaron, and R. D. Amado, Phys. Rev. 124, 1258 (1961).
- <sup>42</sup>S. K. Adhikari and R. D. Amado, Phys. Rev. C 15, 498 (1977); S. K. Adhikari, *ibid.* 17, 903 (1978).